Environmental Science & Technology

Article

Cite This: Environ. Sci. Technol. 2018, 52, 4574−4582

pubs.acs.org/est

On-Road Chemical Transformation as an Important Mechanism of NO_2 Formation

Bo Yang,[†] K. Max Zhang,*[,†] W. David Xu,[†] Shaojun Zhang,[†] Stuart Batterman,[‡] Richard W. Baldauf,[§,∥] Parikshit Deshmukh,[⊥] Richard Snow,[§] Ye Wu,[#,⊗] Qiang Zhang,[#] Zhenhua Li,[#] and Xian Wu[#]

[†]Sibley School of Mechanical and Aerospace Engineering, Cornell University, Ithaca, New York 14853, United States

[‡]School of Public Health, University of Michigan, Ann Arbor, Michigan 48109, United States

[§]U.S. Environmental Protection Agency, Office of Research and Development, National Risk Management Research Laboratory, Research Triangle Park, North Carolina 27711, United States

[∥]U.S. EPA, Office of Transportation and Air Quality, National Vehicle and Fuels Emissions Laboratory, Ann Arbor, Michigan 48105, United States

[⊥]Jacobs Technology, Inc., Durham, North Carolina 27713, United States

[#]School of Environment, State Key Joint Laboratory of Environment Simulation and Pollution Control, Tsinghua University, Beijing 100084, P. R. China

[⊗]State Environmental Protection Key Laboratory of Sources and Control of Air Pollution Complex, Beijing 100084, P. R. China

Supporting Information

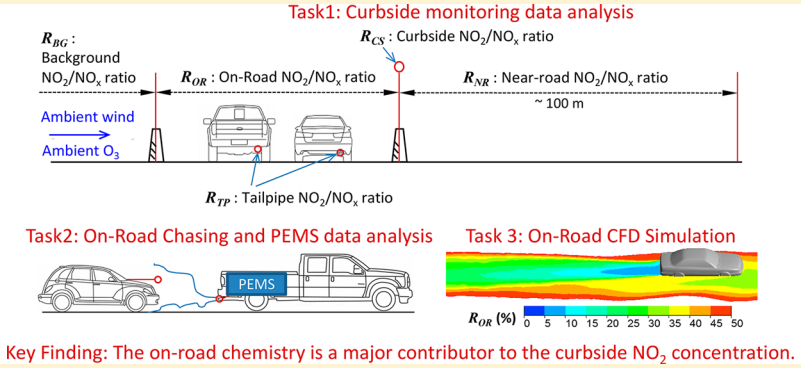

ABSTRACT: Nitrogen dioxide (NO_2) not only is linked to adverse effects on the respiratory system but also contributes to the formation of ground-level ozone (O_3) and fine particulate matter ($PM_{2.5}$). Our curbside monitoring data analysis in Detroit, MI, and Atlanta, GA, strongly suggests that a large fraction of NO_2 is produced during the "tailpipe-to-road" stage. To substantiate this finding, we designed and carried out a field campaign to measure the same exhaust plumes at the tailpipe-level by a portable emissions measurement system (PEMS) and at the on-road level by an electric vehicle-based mobile platform. Furthermore, we employed a turbulent reacting flow model, CTAG, to simulate the on-road chemistry behind a single vehicle. We found that a three-reaction ($NO-NO_2-O_3$) system can largely capture the rapid NO to NO_2 conversion (with time scale ≈ seconds) observed in the field studies. To distinguish the contributions from different mechanisms to near-road NO_2, we clearly defined a set of NO_2/NO_x ratios at different plume evolution stages, namely tailpipe, on-road, curbside, near-road, and ambient background. Our findings from curbside monitoring, on-road experiments, and simulations imply the on-road oxidation of NO by ambient O_3 is a significant, but so far ignored, contributor to curbside and near-road NO_2.

INTRODUCTION

The transportation sector contributes about 30−40% of the emitted nitrogen oxides (NO_x),[1,2] and the health effects of nitrogen dioxide (NO_2) are a public health concern worldwide.[3−6] As part of the revised the National Ambient Air Quality Standards (NAAQS), the U.S. Environmental Protection Agency (USEPA) established monitoring requirements in urban areas to measure NO_2 levels within 50 m of major roads as part of the NO_2 NAAQS. In Europe, NO_2 is one of the major contributors to urban air quality problems and has been routinely monitored in the near-road or street canyon environments.[3] The European Environment Agency estimated 71,000 premature deaths due to NO_2 exposure in Europe,

Received: November 15, 2017
Revised: March 8, 2018
Accepted: March 22, 2018
Published: March 22, 2018

DOI: 10.1021/acs.est.7b05648
Environ. Sci. Technol. 2018, 52, 4574−4582

higher than the estimated mortality caused by ground-level ozone (O_3).[3] From around 1990 onward, the total emissions of NO_x declined significantly in Europe by ~56%,[1] but roadside concentrations of NO_2 declined much less than expected.[7] Approximately 94% of exceedances of the European NO_2 annual limit were observed at traffic monitoring sites.[3] In China, ambient NO_2 concentrations in some megacities (e.g., Beijing, Shanghai) have persisted and exceeded the annual standard limit even though the concentrations of other gaseous pollutants have decreased significantly during the same period.[3,8,9] Even though China does not have a nationwide near-road air quality monitoring network, recently released near-road concentrations well exceed the current standard (e.g., an average exceedance of 20 to 30 $\mu g\ m^{-3}$ for five near-road sites in Beijing).[10] Furthermore, besides being a criteria pollutant itself, NO_2 is also widely adopted as a marker for traffic-related air pollution in health studies.[11−13] For example, positive associations of NO_2 with mortality suggest that traffic pollution relates to premature death.[14]

In the complex roadway environments, direct tailpipe NO_2 emissions, secondary NO_2 through on-road and near-road NO_x titration and background NO_2 all lead to near-road NO_2. Therefore, a better understanding of the contributions from different pathways to near-road NO_2 is necessary for not only effective air quality management, but also evaluating the role of NO_2 as a marker in health studies, as near-road NO_2 could be dominated by different pathways at different conditions.

Moreover, the NO_2/NO_x ratio (typically by volume) is a widely used parameter in air quality management due to its applicability across the scales, from tailpipes to ambient environments. Both highway dispersion modeling (for NO_2) and regional air quality modeling (for O_3, $PM_{2.5}$, etc.) require inputs of NO_2/NO_x ratios, and previous studies have shown that both types of modeling are sensitive to those inputs.[15,16] Thus, another major motivation for our study is to elucidate the physical and chemical processes governing near-road NO_2 in order to provide appropriate NO_2/NO_x ratios for highway dispersion and regional air quality modeling efforts.

To facilitate the subsequent discussions, it is necessary to clearly define NO_2/NO_x ratios at different stages of plume evolution, listed in Table 1. The tailpipe NO_2/NO_x ratio (R_{TP}), also called the primary NO_2/NO_x emission ratio, is defined as the NO_2/NO_x ratio at the vehicle tailpipe exit. R_{TP} for gasoline vehicles is typically around 5% or lower[17,18] but can be higher for diesel vehicles equipped with diesel particulate filters (DPF).[19−21] The curbside NO_2/NO_x ratio, R_{CS}, is defined as the ratio at the edge of roadways. We further define the ratio between the tailpipe exit and the curbside as the on-road NO_2/NO_x ratio, R_{OR}. The ratio in the near-road environments (from the curbside to ~100 m) is defined as near-road NO_2/NO_x ratio, R_{NR}. Lastly, the ratio in the ambient environments is defined as background (or ambient) NO_2/NO_x ratio, R_{BG}.

Table 1. Defined NO_2/NO_x Ratio at Different Locations in a Traffic Environment

location	NO_2/NO_x ratio	description
tailpipe exit	R_{TP}	NO_2/NO_x ratio at the tailpipe exit, also called the primary NO_2/NO_x ratio, which can be measured by emission testing.
on-road	R_{OR}	NO_2/NO_x ratios on the roadway, from the tailpipe to the curbside
curbside	R_{CS}	NO_2/NO_x ratio at the curbsides
near-road	R_{NR}	NO_2/NO_x ratio from the curbside to about 100 m away from the roadways
background	R_{BG}	NO_2/NO_x ratio from the upwind direction or in the ambient environments

It is well recognized that NO_x transforms chemically from NO to NO_2 through titration of O_3 in the near-road environment, resulting in R_{NR} differing from R_{CS}. The near-road chemical transformation has been observed in several field studies.[22−25] In our previous study, we estimated R_{CS} to be ~20−40% based on near-road monitoring data collected at several Texas roadways in the summer of 2007.[16] The roadways studied had low diesel traffic, and the penetration of diesel particulate filters was very low in 2007. Therefore, the relatively high R_{CS} must be explained by mechanisms in addition to the presence of diesel traffic.

This study aims to investigate the physiochemical mechanisms that lead to enhanced curbside NO_2/NO_x ratios (R_{CS}). We posit that on-road (i.e., "tailpipe-to-road"[26]) chemical reactions are a major contributor to NO_2 production, resulting in an evolution from R_{TP} to R_{OR} and to R_{CS}. To our knowledge, on-road chemical transformation of NO_x has not been explicitly studied. However, several recent studies have implicitly indicated the significant role of on-road NO_2 production. The curbside measurements of NO, NO_2 and O_3 in street-canyon environments at two German cities showed that secondary NO_2 production was responsible for a major fraction of measured NO_2.[27] One can deduce from the study that the referred production of NO_2 most likely took place on the streets. Another study of near-road monitoring data at Las Vegas, NV, indicated the R_{CS} ranging from 0.25 to 0.35, substantially higher than the anticipated R_{TP},[28] which we argue can potentially be explained by the on-road production of NO_2. Even though the term "on-road" NO_2/NO_x ratio was used in the Las Vegas study,[28] a close examination of the reported methodology suggested that the term was referred to R_{CS} according to our definition.

In this study, we present the supporting evidence from (1) curbside monitoring near two major highways in Detroit, MI, and Atlanta, GA, respectively, (2) an on-road field experiment in Research Triangle Park (RTP), NC, and (3) on-road simulations using a turbulent reacting flow model. This work is intended to improve future modeling of near-road NO_2 concentrations, air quality and transportation management, and health studies on traffic-related pollutants.

CURBSIDE MONITORING

Site Description and Field Measurements. *Detroit, MI.* Field measurements were performed at several monitoring sites in Detroit, MI, including the Eliza Howell near-road sites, starting fall 2010 and concluded in late summer 2011. For this study, we used data collected between September 2010 and June 2011, when the traffic and meteorological conditions were both well characterized. These sites were originally deployed as part of the Federal Highway Administration (FHWA) and USEPA National Near-Road Study for a one-year period, then continued by the Michigan Department of Environmental Quality (MDEQ) to the present. Data from these sites have being used in the Near-Road Exposures and Effects of Urban Air Pollutants Study (NEXUS), which examined the relationship between near-roadway exposures to air pollutants and respiratory outcomes in a cohort of asthmatic children who live close to major roadways in Detroit, Michigan.[29]

DOI: 10.1021/acs.est.7b05648
Environ. Sci. Technol. 2018, 52, 4574−4582

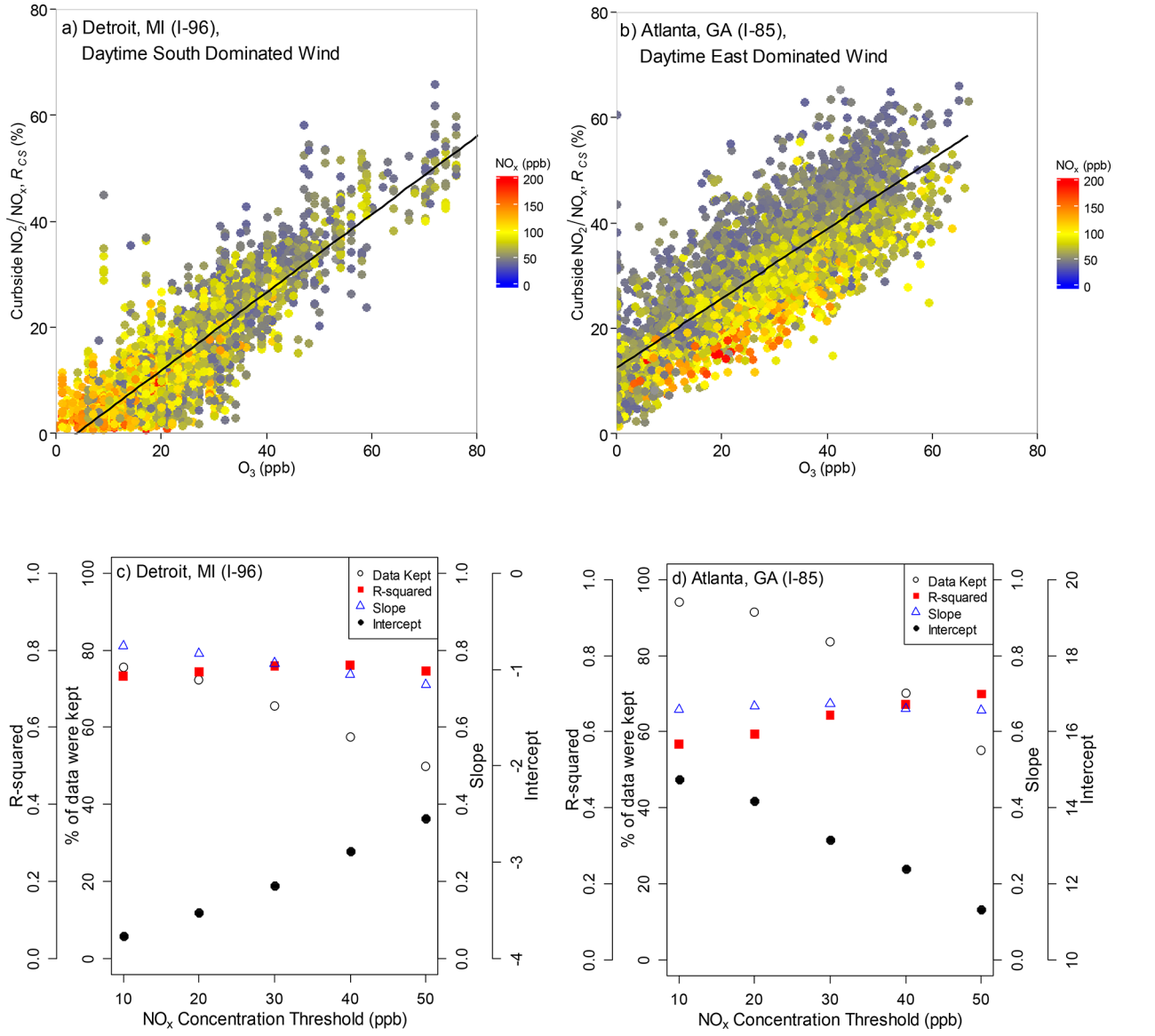

Figure 1. Curbside NO_2/NO_x ratio (R_{CS}) vs ambient O_3 concentrations (ppb) with net NO_x threshold 40 ppb at (a) Detroit, MI (I-96), during the daytime and south dominated wind ($101.25 < \theta < 258.75$) and; (b) Atlanta, GA (I-85), during the daytime and east dominated wind ($11.25 < \theta < 168.75$). Linear regression parameters (slope, intercept and R^2) of the R_{CS} vs O_3 relationships and the amount of data included (as percentage of the total data available) as functions of net NO_x concentration thresholds for (c) Detroit, MI (I-96), and (d) Atlanta, GA (I-85).

The Eliza Howell 1 monitoring site (**EH1**; 42°23′09.6″N, 83°15′58.9″W) is placed at the curbside of Interstate I-96/ Jeffries Freeway (Figure S1a in the Supporting Information (SI)). On the opposite side, site EH4 is located ∼100 m south of I-96, which served as an upwind site when EH1 was downwind of I-96, and allowed us to quantify the contribution of background NO and NO_2 to those measured at EH1. The immediate area is mostly open parkland with some trees and playing fields; surrounding areas are mostly low-rise commercial and residential buildings.

$NO/NO_2/NO_x$ were measured at a height of 3 m using chemiluminescence (Teledyne ML9841B Nitrogen Oxides Analyzer),[30] which reports NO_2 as the difference between NO_x and NO. Wind speed and wind direction were measured at a height of 10 m. Both NO_x and surface meteorology were also measured at EH4. Hourly ozone (O_3) measurements from the Allen Park (AP) site (AQS Site ID: 261630001; 42°13′43.0″N, 83°12′29.9″W), located ∼18.5 km south of EH1 and ∼200 m southeast from the closest major roadway (I-75), were obtained from the USEPA Air Quality System (www.epa.gov/ttn/airs/airsaqs/). A closer O_3 measurement site, E7Mile (AQS Site ID: 261630019; 42°25′50.9″N, 83°00′01.0″W), was not selected due to more than three months missing data between September 2010 and June 2011.

Traffic on I-96 is normally free-flowing with an established speed of 70 mph for cars and 65 mph for trucks. The annual average daily traffic (AADT) on this I-96 segment are 155,000.[30] Based on vehicle classification data measured during the study period at the EH1 site (using radar to classify vehicle size), the percentage of heavy-duty diesel trucks (HDDT) for every 5 min averaged ∼3.0%.

Atlanta, GA. Continuous air quality monitoring data of NO, NO_2, and O_3 were obtained at two sites in Atlanta, GA: a curbside site off Interstate I-85 near Georgia Institute of Technology (NRGT; AQS Site ID: 13-121-0056; 33°46′41.934″ N, 84°23′29.1048″ W) and a background site

DOI: 10.1021/acs.est.7b05648
Environ. Sci. Technol. 2018, 52, 4574−4582

in South DeKalb (SDK; AQS Site ID: 13-089-0002; 33°41′16.692″ N, 84°17′25.7280″ W), about 13.5 km southeast from the NRGT site. Figure S1b in the SI depicts the locations of the two sites. The monitoring at NRGT started near the end of May 2014. We analyzed data collected between January 2015 and March 2017 since minute-level data of of NO, NO_2, and O_3 from both NRGT and SDK are available during this period.

I-85 is a major interstate freeway that runs northeast−southwest in Georgia. The AADT on this segment is ∼332,000 in 2015, and ∼353,700 in 2016, accordingly to the closest traffic monitoring station (ID: 1215481; 33°46′23.8800″ N, 84°23′24.0000″ W) (http://trafficserver.transmetric.com/gdot-prod/tcdb.jsp?siteid=1215481). The truck percentage is ∼3.7% based on another nearby station (ID: 1216118; 33°46′32.88″ N, 84°23′24.72″ W) (http://trafficserver.transmetric.com/gdot-prod/tcdb.jsp?siteid=1216118).

Curbside Data Analysis. To investigate the role of on-road chemical transformation of NO_x, we screened the Detroit data using the following criteria: First, we selected daytime data (6AM-6PM) under south-dominant wind conditions ($101.25 < \theta < 258.75$, θ is the wind direction in degrees) so that EH1 was downwind of I-96. Next, we subtracted the upwind NO_2 and NO_x concentrations (i.e., at EH4) from the corresponding values at EH1, thus reflecting the net contributions of highway emissions. Finally, we set a net NO_x concentration threshold to ensure the curbside data reflect the highway influence. In other words, the curbside NO_x concentrations are expected to be higher than the upwind NO_x concentrations. The higher the threshold value, the more confident we are of the highway influence, given the uncertainties and detection limits in the NO_x measurements. But the same time, a higher threshold value may also exclude some low-traffic conditions. We tested the sensitivity of our results to the net NO_x concentration threshold. We followed similar steps to analyze the Atlanta data. First, we selected daytime data (8AM-5PM) under east-dominant wind conditions ($11.25 < \theta < 168.75$) so that NRGT was downwind of I-85. Next, we subtracted the ambient NO_2 and NO_x concentrations (i.e., at SDK) from the corresponding values at NRGT to reflect the net contributions of highway emissions. We also tested the sensitivity of net NO_x concentration thresholds.

Figure 1 summarizes the main findings from our curbside analysis of the Detroit and Atlanta data sets. The relationships between net curbside NO_2/NO_x ratios (R_{CS}) and ambient O_3 concentrations (with net NO_x concentrations represented by color scales) are illustrated in Figure 1a,b for Detroit and Atlanta, respectively. The overall linear relationships between O_3 concentrations and net R_{CS} from these two curbside measurements support the significance of on-road chemical transformation. In other words, higher ambient O_3 concentrations, once mixed with highway emissions, convert NO to NO_2 during the tailpipe-to-road process. Conversely, if the role of on-road chemical transformation was insignificant, then net R_{CS} would not show a relationship with O_3 concentrations.

Parts c and d of Figure 1 depict the sensitivities of linear regression parameters (slope, intercept, and R^2 as shown in Figure 1a,b) and the amount of data included (as percentage of the total data available) to the different net NO_x concentration thresholds, ranging from 10 to 50 ppb. As expected, the percentage of data included decreases with the net NO_x threshold for both highways. At the 10 ppb threshold, around 76% data are included in Detroit, MI, and 94% data were kept in Atlanta, GA. At the 50 ppb threshold, both of the two data sets dropped to around 50%. However, the slopes from both data sets appear not sensitive to the net NO_x threshold, only changing from 0.71 to 0.81 for Detroit and from 0.66 to 0.73 for Atlanta, respectively. The R^2 values for Detroit, varying from 0.73 to 0.76, were not sensitive to the NO_x threshold, while those for Atlanta were more sensitive to the threshold, increasing from 0.57 to 0.70 as the NO_x threshold increases from 10 to 50 ppb. Parts a and b of Figures 1 were both plotted at 40 ppb net NO_x threshold to achieve a balance of high percentage data inclusion and high R^2.

The intercepts for Detroit and Atlanta both appear to be sensitive to the NO_x threshold, but with opposite directions. Physically, the intercepts represent the tailpipe NO_2/NO_x ratios, R_{TP}. The intercepts for Detroit are negative (albeit small in magnitude), approaching positive values as the NO_x threshold increases. The intercepts for Atlanta are positive, starting with relative large magnitude, e.g., 15% when the NO_x threshold is set to 10 ppb and decreasing to ∼11% at the 50 ppb net NO_x threshold. One contributing factor to the negative intercepts in Detroit was found to be associated with the traffic patterns. Figure 1a indicates high NO_x conditions predominately appear when ambient O_3 concentrations are low, which represented the early morning and late afternoon traffic peaks. Those high-NO_x and low-O_3 conditions lead to a small fraction of NO being converted and thus low NO_2/NO_x ratios. The clustering of data points of low NO_2/NO_x ratios and low O_3 concentrations pushes the linear regression toward the negative intercept side. By contrast, high NO_x conditions are evenly distributed at the NGRT site across the whole range of O_3 concentrations, suggesting a weak diurnal traffic pattern. It is worth noting that I-85 segment near NRGT is one of the most trafficked highways in the U.S.

Figure 1a raises the question over the contribution of on-road chemistry to curbside NO_2 concentrations in Detroit since conditions with high net R_{CS} and high ambient O_3 appear when net NO_x concentrations are relatively low. Figure S2 in the SI illustrates the relationship between net NO_2 concentrations (i.e., from both primary NO_2 emissions and on-road chemical transformation) and ambient O_3 from the Detroit data set, which presents a positive linear trend and implies a significant contribution from on-road chemical transformation to curbside NO_2 concentrations. Furthermore, Figure 1b (based on the Atlanta data) corroborates this conclusion as conditions with high net R_{CS} and high ambient O_3 appear with high net NO_x concentrations (thus high net NO_2 concentrations). Moreover, Figure S3 in the SI depicted the relationships between R_{CS} and solar radiation at different ambient O_3 concentrations. The results suggest that R_{CS} is not very sensitive to the NO_2 photolysis rates (with solar radiation as a surrogate), which in turn indicates that the titration of O_3 by NO is the dominant reaction. Future studies are needed to conduct detailed analysis of the contributions from different pathways (such as ambient background, tailpipe or primary NO_2 emissions, on-road chemistry, near-road chemistry) to curbside/near-road NO_2 concentrations.

We acknowledge the uncertainties in the curbside data analysis. For example, the NRGT does not have a near-road upwind site for us to reliably estimate net NO_x contributions, which at least partially explain why the regression parameters are much more sensitive to the net NO_x threshold in Atlanta than Detroit. In addition, we did not have near-road upwind O_3 measurements for either Detroit or Atlanta. Several studies reported spatial variations of O_3 concentrations in urban

DOI: 10.1021/acs.est.7b05648
Environ. Sci. Technol. 2018, 52, 4574−4582

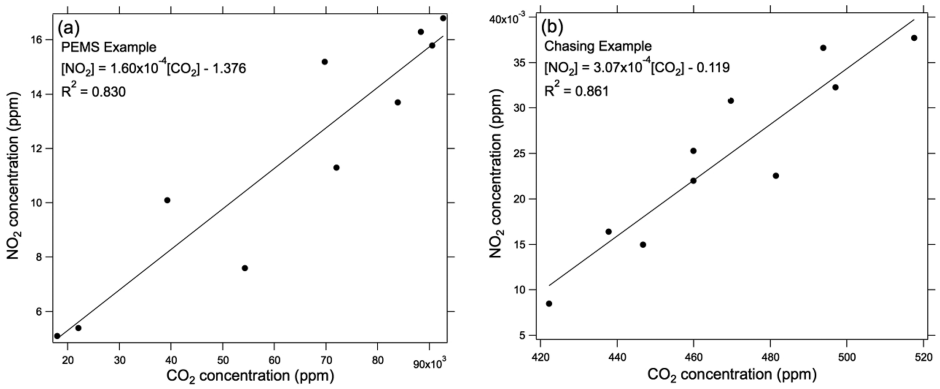

Figure 2. One pair of synchronized plume signals of NO_2 vs CO_2 concentrations based on (a) on-road chasing measurement and (b) tailpipe-level PEMS measurement for deriving CO_2-normalized NO_2 concentrations.

areas.[31−33] The O_3 concentrations measured at the ambient sites may not accurately represent the near-road upwind conditions. Nevertheless, the curbside data from two different highways showed very consistent trends. Together, the curbside analysis provides strong evidence for the significant role of on-road NO_x transformation.

■ ON-ROAD EXPERIMENT

Field Measurements. Motivated by the finding from the curbside data analysis described earlier, we designed an on-road field campaign to gather further evidence on the on-road NO_x chemical transformation. The overall concept of the on-road experiment was to measure the same exhaust plumes both at the tailpipe-level by Portable Emissions Monitoring System (PEMS) and at the on-road level (after initial dilution) by a mobile chasing platform. Then we would expect to observe noticeable differences in the tailpipe-level and on-road level NO_2/NO_x ratios with significant on-road NO_x chemical transformation. However, it is technically challenging to directly measure on-road NO_2/NO_x ratios (R_{OR}) because reliable, fast-responding instruments for NO (or NO_x) are not readily available. Wild and co-workers recently developed a fast-responding instrument via Cavity Ring-Down Spectroscopy.[34] But we did not have access to that instrument. As an alternative, our analysis relied on CO_2 and NO_2 by defining CO_2-normalized NO_2 concentration as $\Delta NO_2/\Delta CO_2$, essentially using CO_2 as a dilution indictor, for PEMS and mobile platform measurements, respectively. Details for this analysis are provided later.

In our experiment, we employed an electric vehicle-based mobile platform equipped with air quality analyzers at 1 s sampling intervals to conduct the on-road chasing measurements, capturing the on-road concentrations of CO_2 (Quantum Cascade Laser, Aerodyne Research, Inc.) and NO_2 (Cavity Attenuation Phase Shift, Aerodyne Research, Inc.). The sampling probe was positioned at the bottom front of the mobile platform, around the same height as the exhaust tailpipe of the vehicle being followed. We detected a six-second delay in response due to the sampling line, and this delay was accounted for in the subsequent data analysis. The chasing routes were recorded using a high-precision GPS unit (Crescent R100, Hemisphere GPS). A webcam was operated in the front seat of the mobile monitoring vehicle and recorded the traffic conditions continuously during the on-road measurements.

The vehicle being chased (referred to as "target vehicle") was a 2003 Ford F350 diesel powered truck (engine displacement 6.0 L, 8 cylinders, ∼ 53,000 miles, 7940 lbs actual weight). Tailpipe-level CO_2 and NO_2 concentrations were measured using a Portable Emissions Monitoring System (PEMS) (SEMTECH Ecostar; Sensors, Inc.). The PEMS samples directly from the subject vehicle's raw exhaust and is capable of providing on-board CFR 1065 compliant emissions determinations at a rate of 1 Hz as the subject vehicle is being operated on the highway. The PEMS utilizes a nondispersive infrared (NDIR) sensor for CO_2 measurements and a nondispersive ultraviolet (NDUV) sensor for NO_2 measurements.

The on-road field campaign took place from February 22nd until March 4th, 2016 in Research Triangle Park (RTP), NC. The measurements conducted in the afternoon of February 29 (FEB29PM), the morning of March 1 (MAR01AM), and the afternoon of March 1 (MAR01PM) focused on comparing PEMS and on-road chasing results.

On-Road Data Analysis. We started the data analysis by screening the videos recorded during the experiment to select the time segments without the presence of heavy duty vehicles around the target vehicle. Emissions from heavy duty vehicles may distort the on-road chasing results. For the selected time segments, we processed the chasing data using 2 s average to remove noise in the raw 1 s data.

Then a two-step synchronization was adopted to further process the data. The first-step was to synchronize the chasing CO_2 and NO_2 signals, which usually required 1-s or 2-s time shift in time series, to identify synchronized CO_2 and NO_2 spikes. At the end of the first step, we obtained a series of synchronized CO_2 and NO_2 spikes that captured on-road plume signals with high confidence. The second step was to synchronize chasing plume signals with PEMS data. The distance between the chasing object and the mobile platform was usually within 20 m. Given the exit velocity ∼20 m s^{-1}, the time delay between the PEMS and chasing signals should be ∼1 s. In practice, the acceleration of the truck usually caused a large spike in both PEMS and chasing signals, which helped us to determine the time delay. At the end of the second step, we acquired a list of paired PEMS and chasing signals, representing the same exhaust plumes measured by the two methods.

The CO_2-normalized NO_2 concentration ($\Delta NO_2/\Delta CO_2$) can be visualized by the slope of NO_2 vs CO_2 scatter plots. Figure 2 illustrates how we calculated CO_2-normalized NO_2 concentration using one pair of synchronized plume signals as an example.

DOI: 10.1021/acs.est.7b05648
Environ. Sci. Technol. 2018, 52, 4574−4582

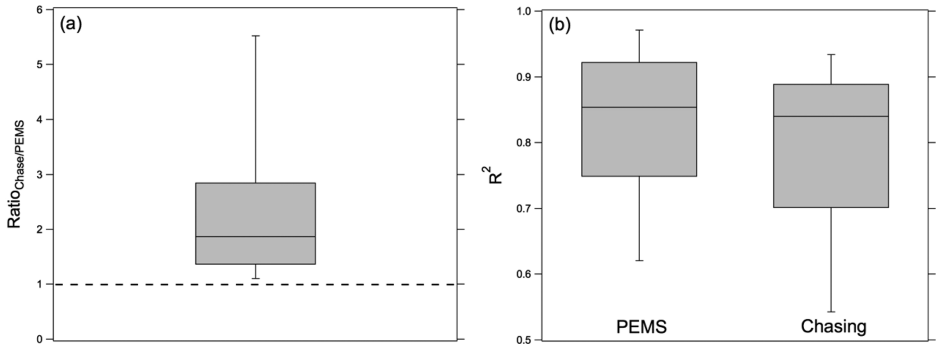

Figure 3. Distributions of (a) $Ratio_{Chase/PEMS}$ (i.e., the ratio of CO_2-normalized NO_2 concentrations from on-road chasing over tailpipe PEMS measurements) and (b) R^2 values for deriving CO_2-normalized NO_2 concentrations from chasing and PEMS measurements. In both (a) and (b), the box represents the middle 50% of the data, extending from the 25th to the 75th percentiles; the horizontal line through the center of the box is the median; the whiskers represent 10th and 90th percentiles.

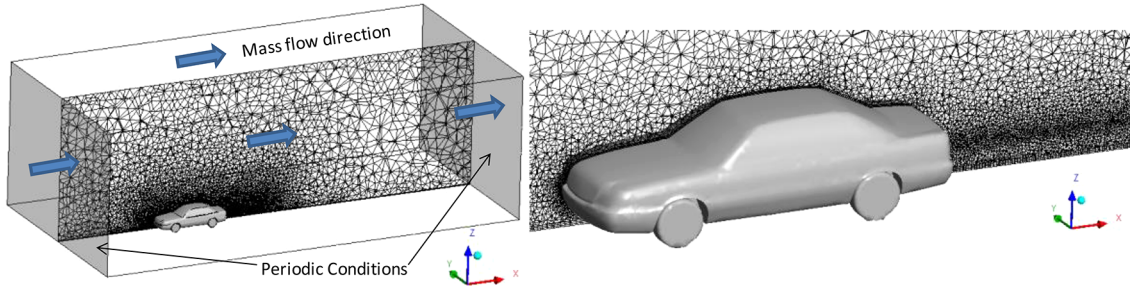

Figure 4. Computational domain and mesh around the car.

We identified a total of 109 synchronized plume signals, and calculated the ratio of CO_2-normalized NO_2 concentrations from on-road chasing over tailpipe PEMS measurements for each plume signal, referred to as $Ratio_{Chase/PEMS}$, i.e., a $Ratio_{Chase/PEMS} > 1$ implies on-road NO_2 production. Figure 3 shows the distributions of this ratio and coefficients of determination (R^2) for the linear regressions (as indicated in Figure 2). $Ratio_{Chase/PEMS} > 1$ for all 109 plume signals with the median value as 1.87, and R^2 values for both PEMS and on-road chasing measurements are high (with the median values over 0.8), suggesting the results are reasonably robust.

In summary, the results from the on-road experiment further indicate the significant role of on-road NO_x chemical transformation.

COUPLED ON-ROAD TURBULENCE AND CHEMISTRY MODELING

Methodology for On-Road Simulations. As the third part of our study, we employed the Comprehensive Turbulent Aerosol Dynamics and Gas Chemistry (CTAG) model to simulate the coupled on-road turbulent mixing and chemistry of individual exhaust plumes to test whether the rapid transformation observed is kinetically feasible under typical on-road conditions. CTAG is an appropriate model for this purpose as it was designed to simulate transport and transformation of multiple air pollutants, e.g., from emission sources to ambient background.[35−40]

Shown in Figure 4, the computational domain was constructed based on a single lane with an individual passenger car. The domain dimensions are 30 m (L) × 15 m (W) × 10 m (H). The positive Y direction is the downwind crosswind direction. The geometry of the passenger car was modeled using a realistic shape rather than block shapes.

While full-scale simulations with detailed site-specific conditions (e.g., capturing multiple vehicles corresponding to traffic mix, highway geometry, etc.) are beyond the scope of this paper, we utilized the environmental conditions captured in the Detroit data set to set up the simulations. The velocity inlet boundary was specified on the left and top sides of the domain to simulate the ambient south crosswind speed. The periodic boundary conditions with the flow rate based on vehicle speed (70 mph or 31.3 m s^{-1} as in the I-96 segment), specified on both ends of the computational domain, was adopted to represent the continuous traffic flow. The passenger car's tailpipe, 60 mm in diameter, is parallel to the road and specified as a mass flow inlet with a total mass flow rate of 0.055 kg s^{-1} and exhaust temperature of 480 K.[41] The tailpipe-level NO_x emission rate was estimated by using EPA's MOtor Vehicle Emission Simulator (MOVES). A NO_2/NO_x volume ratio of 5% was assigned at the tailpipe level (i.e., R_{TP} = 5%). The road surface was modeled as a moving wall at the vehicle speed, thus representing the relative motion between the vehicle and the road. Ambient background NO_x and NO_2 concentrations for each case are specified based on the Detroit data (EH4).

We modeled the dispersion and chemical reactions using steady-state Reynolds averaged Navier−Stokes (RANS) turbulence model to simulate the flow fields and species transport. The finite rate (FR) chemical reaction model[42] was coupled with the eddy dissipation method (EDM),[43] referred to as the EDM/FR model, in which turbulence−chemistry interaction is accounted for through the representation of the source term the species transport equations. Both an Arrhenius rate based on the global chemistry mechanism, and a turbulent mixing rate based on the Magnussen−Hjertager expression are estimated.[43] The smaller of the two rates is then used as the source term. We adopted a simplified chemical mechanism

DOI: 10.1021/acs.est.7b05648
Environ. Sci. Technol. 2018, 52, 4574−4582

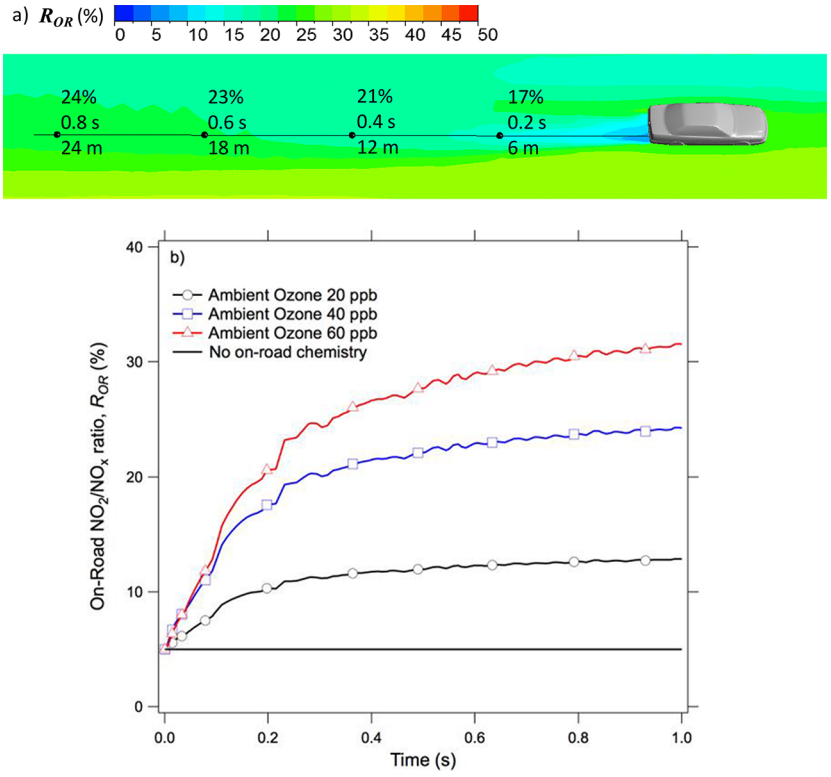

Figure 5. (a) On-road NO_2/NO_x ratio (R_{OR}) contour plot on a horizontal plane at the tailpipe height in the simulation domain illustrated in Figure 4. The ambient ozone concentration is set to be 40 ppb. The black solid line is the tailpipe centerline. Values along the solid line represent the resident time and corresponding R_{OR}. (b) R_{OR} along the tailpipe centerline for different ambient ozone concentrations.

using a four reaction ($NO-NO_2-O_3$) system shown in Table S1 with reaction constants taken from the CB05 mechanism.[44] These reactions have been shown to be dominant in near-source environments.[16,45] The photolysis rate of NO_2 was determined based on our previous work[16] (also described in section S4 of the SI) and average solar radiation at the near-road site in Detroit obtained from the U.S. National Solar Radiation Database. The governing equations of the Realizable k-ε model (one type of RANS models) and the species transport equation are presented in section S2. The mesh resolution sensitivity study is illustrated in Figures S4 and S5.

RESULTS FROM ON-ROAD SIMULATIONS

Figure 5a illustrates the contour of R_{OR} on a horizontal plane at the tailpipe height in the simulation domain (Figure 4) with the ambient ozone concentration set to be 40 ppb. Some representative R_{OR} values are marked in along the tailpipe centerline with the corresponding residence time, estimated by dividing the distance to the tailpipe center by the driving velocity. Figure 5b shows R_{OR} values along the tailpipe centerline as a function of resident time at levels of ambient O_3 concentrations (20, 40, and 60 ppb).

It is revealed from Figure 5 that higher the ambient O_3 concentration leads to higher R_{OR}. As expected, R_{OR} remain nearly a constant if chemical reactions are turned off. Furthermore, the coupled turbulent mixing and simplified $NO-NO_2-O_3$ chemistry can achieve the NO_2 conversion rate similar to the order of magnitude of the observed values, though a direct comparison is not feasible. The values of $Ratio_{Chase/PEMS}$ derived from the on-road experiment are roughly equivalent of changes in NO_2/NO_x ratios. Given the ~1 s transport from the tailpipe of the target vehicle to the probe of the mobile platform, a $Ratio_{Chase/PEMS}$ of 2 suggests doubling of NO_2/NO_x ratios in less than 1 s at ambient O_3 concentration ~40 ppb. The modeling results show that even at relatively low ambient O_3 level (e.g., 20 ppb), R_{OR} can double of R_{TP} in less than 1 s. Figure S6 in the SI illustrates the R_{OR} values along the tailpipe centerline as a function of resident time at different NO_2 photolysis rates with ambient O_3 concentration at 40 ppb. The results suggest that R_{OR} is not sensitive to NO_2 photolysis rates, which further supports NO $+O_3$ as the dominant reaction during the "tailpipe-to-road" stage. As mentioned previously, R_{OR} also depends on the relative amounts of NO_x and O_3. More in-depth studies are needed to explore how different traffic and meteorology conditions affect on-road NO_x transformation.

IMPLICATIONS

Our study has provided experimental evidence, through curbside data analysis and on-road field measurements, that substantial amounts of freshly emitted NO are oxidized to NO_2 during the "tailpipe-to-road" stage. The subsequent modeling analysis indicates that chemical conversion is rapid, and that $NO-NO_2-O_3$ chemistry significantly increases NO_2/NO_x ratios in the on-road environment from the relatively low ratio at the tailpipe. The findings have raised the importance of differentiating NO_2/NO_x ratios at various stages of exhaust plume evolution in order to account for the contributions of primary emissions, on-road chemistry, near-road chemistry and ambient background to near-road NO_2 concentrations. We have shown that on-road chemistry is a major contributor to curbside NO_2, and likely near-road NO_2. In general, $R_{TP} < R_{OR} < R_{CS} < R_{NR}$. The study results have important implications for transportation and air quality management. First, the on-road

DOI: 10.1021/acs.est.7b05648
Environ. Sci. Technol. 2018, 52, 4574−4582

distributions of NO_2/NO_x ratios resulting from chemistry and turbulent mixing challenge a common assumption in all major highway dispersion models that pollutants (as well as NO_2/NOx ratios) are uniformly distributed on and over the highways.[46−48] In practice, this assumption essentially treats $R_{TP} = R_{OR} = R_{CS}$, which has been shown to be invalid by our study and can lead to significant underestimation of near-road NO_2 as assumed R_{TP} are usually taken from tailpipe measurements without accounting for on-road chemistry. Our analysis can potentially lead to a parametrization scheme that accounts for the effects of on-road NO_x chemistry, which provides more accurate inputs for near-road NO_2 modeling and enhance the capability of modeling near-road NO_2 concentrations for regulatory purposes. Second, considering the significant production of NO_2 on roadways, strategies for attaining near-road NO_2 standards need to account for the effects of on-road NO_x chemistry, i.e., not only local tailpipe emissions, but also regional ozone concentrations. Finally, properly representing the effects of on-road chemistry on NO_2 production will also improve the regional O_3 and NO_2 modeling. A regional modeling study in Southeast Texas showed compared to the traditional 5% NO_2/NO_x emission ratio, a higher NO_2/NO_x ratio (29%) could lead to a 6 ppb increase in the 8 h ozone.[15] Another regional air quality study in Europe indicated an up to 8 $\mu g\ m^3$ increase in the annual average NO_2 concentration when the NO_2/NO_x emission ratio is increased from 20 to 70%.[49] Future studies of the joint impact of chemical transformations through on-road chemistry and catalytic chemistry in diesel after treatment devices are needed.

■ ASSOCIATED CONTENT

Supporting Information

The Supporting Information is available free of charge on the ACS Publications website at DOI: 10.1021/acs.est.7b05648.

Curbside data analysis, governing equations, mesh sensitivity, and chemical mechanism and photolysis rate sensitivity in on-road simulations (PDF)

■ AUTHOR INFORMATION

Corresponding Author

*Tel: 607-254-5402. Fax: 607-255-1222. E-mail: kz33@cornell.edu.

ORCID

K. Max Zhang: 0000-0002-3324-6571

Ye Wu: 0000-0002-2176-6174

Author Contributions

The manuscript was written through contributions of all authors. All authors have given approval to the final version of the manuscript.

Notes

The authors declare no competing financial interest.

■ ACKNOWLEDGMENTS

The authors thank Mr. Chad Bailey at the United States Environmental Protection Agency (EPA) for valuable discussions in developing the research idea, Ms. Janet Aldredge and Mr. Daniel Ross at Georgia Department of Natural Resources for providing the air quality data in Atlanta. Research described in this article was conducted under contract to the Health Effects Institute (HEI), an organization jointly funded by the EPA (Assistance Award No. R-82811201) and certain motor vehicle and engine manufacturers. The contents of this article do not necessarily reflect the views of HEI, or its sponsors, nor do they necessarily reflect the views and policies of the EPA or motor vehicle and engine manufacturers. K.M.Z. acknowledges additional support from the National Science Foundation (NSF) through Grant No. 1605407, and S. Batterman acknowledges additional support from the National Institute of Environmental Health Sciences (NIEHS) through Grant No. P30ES017885.

■ REFERENCES

(1) European Environment Agency. *European Union emission inventory report 1990−2015 under the UNECE Convention on Long-range Transboundary Air Pollution (LRTAP)*, 2017.

(2) US Environmental Protection Agency. *2014 National Emissions Inventory (NEI) Data*, 2018.

(3) European Environment Agency. *Air Quality in Europe — 2016 Report*, 2016.

(4) Cesaroni, G.; Badaloni, C.; Gariazzo, C.; Stafoggia, M.; Sozzi, R.; Davoli, M.; Forastiere, F. Long-term exposure to urban air pollution and mortality in a cohort of more than a million adults in Rome. *Environ. Health Perspect.* **2013**, *121* (3), 324.

(5) Chauhan, A. J.; Inskip, H. M.; Linaker, C. H.; Smith, S.; Schreiber, J.; Johnston, S. L.; Holgate, S. T. Personal exposure to nitrogen dioxide (NO2) and the severity of virus-induced asthma in children. *Lancet* **2003**, *361* (9373), 1939−1944.

(6) Liu, J. C.; Peng, R. D. Health effect of mixtures of ozone, nitrogen dioxide, and fine particulates in 85 US counties. *Air Qual., Atmos. Health* **2018**, 1−14.

(7) Grange, S. K.; Lewis, A. C.; Moller, S. J.; Carslaw, D. C. Lower vehicular primary emissions of NO2 in Europe than assumed in policy projections. *Nat. Geosci.* **2017**, *10* (12), 914.

(8) Shanghai Environmental Protection Bureau. *Shanghai Environmental Bulletin 2016*, 2017.

(9) United Nations Environment Programme. *A Review of Air Pollution Control in Beijing: 1998−2013*, 2016.

(10) Beijing Municipal Environmental Monitoring Center. *Beijing Air Quality Data in 2015−2016*, 2016.

(11) Castro-Giner, F.; Künzli, N.; Jacquemin, B.; Forsberg, B.; de Cid, R.; Sunyer, J.; Jarvis, D.; Briggs, D.; Vienneau, D.; Norback, D. Traffic-related air pollution, oxidative stress genes, and asthma (ECHRS). *Environ. Health Perspect.* **2009**, *117* (12), 1919.

(12) Finkelstein, M. M.; Jerrett, M. A study of the relationships between Parkinson's disease and markers of traffic-derived and environmental manganese air pollution in two Canadian cities. *Environ. Res.* **2007**, *104* (3), 420−432.

(13) Freire, C.; Ramos, R.; Puertas, R.; Lopez-Espinosa, M.-J.; Julvez, J.; Aguilera, I.; Cruz, F.; Fernandez, M.-F.; Sunyer, J.; Olea, N. Association of traffic-related air pollution with cognitive development in children. *Journal of Epidemiology & Community Health* **2010**, *64* (3), 223−228.

(14) Jerrett, M.; Burnett, R. T.; Beckerman, B. S.; Turner, M. C.; Krewski, D.; Thurston, G.; Martin, R. V.; van Donkelaar, A.; Hughes, E.; Shi, Y. Spatial analysis of air pollution and mortality in California. *Am. J. Respir. Crit. Care Med.* **2013**, *188* (5), 593−599.

(15) Kota, S. H.; Ying, Q.; Zhang, Y. Simulating near-road reactive dispersion of gaseous air pollutants using a three-dimensional Eulerian model. *Sci. Total Environ.* **2013**, *454−455*, 348−357.

(16) Wang, Y. J.; DenBleyker, A.; McDonald-Buller, E.; Allen, D.; Zhang, K. M. Modeling the chemical evolution of nitrogen oxides near roadways. *Atmos. Environ.* **2011**, *45* (1), 43−52.

(17) Wild, R. J.; Dubé, W. P.; Aikin, K. C.; Eilerman, S. J.; Neuman, J. A.; Peischl, J.; Ryerson, T. B.; Brown, S. S. On-road measurements of vehicle NO2/NOx emission ratios in Denver, Colorado, USA. *Atmos. Environ.* **2017**, *148*, 182−189.

DOI: 10.1021/acs.est.7b05648
Environ. Sci. Technol. 2018, 52, 4574−4582

(18) Heeb, N. V.; Saxer, C. J.; Forss, A.-M.; Brühlmann, S. Trends of NO-, NO 2-, and NH 3-emissions from gasoline-fueled Euro-3-to Euro-4-passenger cars. *Atmos. Environ.* **2008**, *42* (10), 2543−2554.
(19) May, A. A.; Nguyen, N. T.; Presto, A. A.; Gordon, T. D.; Lipsky, E. M.; Karve, M.; Gutierrez, A.; Robertson, W. H.; Zhang, M.; Brandow, C. Gas-and particle-phase primary emissions from in-use, on-road gasoline and diesel vehicles. *Atmos. Environ.* **2014**, *88*, 247−260.
(20) Misra, C.; Ruehl, C.; Collins, J.; Chernich, D.; Herner, J. In-Use NOx Emissions from Diesel and Liquefied Natural Gas Refuse Trucks Equipped with SCR and TWC, Respectively. *Environ. Sci. Technol.* **2017**, *51* (12), 6981−6989.
(21) Thiruvengadam, A.; Besch, M.C.; Thiruvengadam, P.; Pradhan, S.; Carder, D.; Kappanna, H.; Gautam, M.; Oshinuga, A.; Hogo, H.; Miyasato, M. Emission rates of regulated pollutants from current technology heavy-duty diesel and natural gas goods movement vehicles. *Environ. Sci. Technol.* **2015**, *49* (8), 5236−5244.
(22) Clements, A. L.; Jia, Y.; Denbleyker, A.; McDonald-Buller, E.; Fraser, M. P.; Allen, D. T.; Collins, D. R.; Michel, E.; Pudota, J.; Sullivan, D.; Zhu, Y. Air pollutant concentrations near three Texas roadways, part II: Chemical characterization and transformation of pollutants. *Atmos. Environ.* **2009**, *43* (30), 4523−4534.
(23) Baldauf, R. W.; Heist, D.; Isakov, V.; Perry, S.; Hagler, G. S.; Kimbrough, S.; Shores, R.; Black, K.; Brixey, L. Air quality variability near a highway in a complex urban environment. *Atmos. Environ.* **2013**, *64*, 169−178.
(24) Kimbrough, S.; Baldauf, R. W.; Hagler, G. S.; Shores, R. C.; Mitchell, W.; Whitaker, D. A.; Croghan, C. W.; Vallero, D. A. Long-term continuous measurement of near-road air pollution in Las Vegas: seasonal variability in traffic emissions impact on local air quality. *Air Qual., Atmos. Health* **2013**, *6* (1), 295−305.
(25) Richmond-Bryant, J.; Owen, R. C.; Graham, S.; Snyder, M.; McDow, S.; Oakes, M.; Kimbrough, S. Estimation of on-road NO2 concentrations, NO2/NOX ratios, and related roadway gradients from near-road monitoring data. *Air Qual., Atmos. Health* **2017**, *10* (5), 611−625.
(26) Zhang, K. M.; Wexler, A. S. Evolution of particle number distribution near roadways—Part I: analysis of aerosol dynamics and its implications for engine emission measurement. *Atmos. Environ.* **2004**, *38* (38), 6643−6653.
(27) Kurtenbach, R.; Kleffmann, J.; Niedojadlo, A.; Wiesen, P. Primary NO2 emissions and their impact on air quality in traffic environments in Germany. *Environ. Sci. Eur.* **2012**, *24* (1), 21.
(28) Richmond-Bryant, J.; Owen, R. C.; Graham, S.; Snyder, M.; McDow, S.; Oakes, M.; Kimbrough, S. Estimation of on-road NO2 concentrations, NO2/NOX ratios, and related roadway gradients from near-road monitoring data. *Air Qual., Atmos. Health* **2017**, *10* (5), 611−625.
(29) Vette, A.; Burke, J.; Norris, G.; Landis, M.; Batterman, S.; Breen, M.; Isakov, V.; Lewis, T.; Gilmour, M. I.; Kamal, A.; Hammond, D.; Vedantham, R.; Bereznicki, S.; Tian, N.; Croghan, C. The Near-Road Exposures and Effects of Urban Air Pollutants Study (NEXUS): Study design and methods. *Sci. Total Environ.* **2013**, *448*, 38−47.
(30) Michigan Department of Environmental Quality. *Michigan's 2013 Ambient Air Monitoring Network Review*; 2012.
(31) Karl, T. *Spatial variability of ozone and other pollutants at St. Louis, Missouri*; Environmental Protection Agency, Environmental Sciences Research Lab. Research Triangle Park, NC, 1979.
(32) Lin, C.; Feng, X.; Heal, M. R. Temporal persistence of intra-urban spatial contrasts in ambient NO2, O3 and Ox in Edinburgh, UK. *Atmos. Pollut. Res.* **2016**, *7* (4), 734−741.
(33) Mulholland, J. A.; Butler, A. J.; Wilkinson, J. G.; Russell, A. G.; Tolbert, P. E. Temporal and spatial distributions of ozone in Atlanta: regulatory and epidemiologic implications. *J. Air Waste Manage. Assoc.* **1998**, *48* (5), 418−426.
(34) Wild, R. J.; Edwards, P. M.; Dubé, W. P.; Baumann, K.; Edgerton, E. S.; Quinn, P. K.; Roberts, J. M.; Rollins, A. W.; Veres, P. R.; Warneke, C.; Williams, E. J.; Yuan, B.; Brown, S. S. A Measurement of Total Reactive Nitrogen, NOy, together with NO2, NO, and O3 via Cavity Ring-down Spectroscopy. *Environ. Sci. Technol.* **2014**, *48* (16), 9609−9615.
(35) Wang, Y.; Zhang, K. M. Modeling near-road air quality using a computational fluid dynamics (CFD) model, CFD-VIT-RIT. *Environ. Sci. Technol.* **2009**, *43* (20), 7778−7783.
(36) Wang, Y. J.; Zhang, K. M. Coupled turbulence and aerosol dynamics modeling of vehicle exhaust plumes using the CTAG model. *Atmos. Environ.* **2012**, *59*, 284−293.
(37) Wang, Y. J.; Nguyen, M. T.; Steffens, J. T.; Tong, Z. M.; Wang, Y. G.; Hopke, P. K.; Zhang, K. M. Modeling multi-scale aerosol dynamics and micro-environmental air quality near a large highway intersection using the CTAG model. *Sci. Total Environ.* **2013**, *443*, 375−386.
(38) Wang, Y. J.; Yang, B.; Lipsky, E. M.; Robinson, A. L.; Zhang, K. M. Analyses of Turbulent Flow Fields and Aerosol Dynamics of Diesel Engine Exhaust Inside Two Dilution Sampling Tunnels Using the CTAG Model. *Environ. Sci. Technol.* **2013**, *47* (2), 889−898.
(39) Steffens, J. T.; Heist, D. K.; Perry, S. G.; Isakov, V.; Baldauf, R. W.; Zhang, K. M. Effects of roadway configurations on near-road air quality and the implications on roadway designs. *Atmos. Environ.* **2014**, *94*, 74−85.
(40) Yang, B.; Zhang, K. M. CFD-based turbulent reactive flow simulations of power plant plumes. *Atmos. Environ.* **2017**, *150*, 77−86.
(41) Uhrner, U.; von Löwis, S.; Vehkamäki, H.; Wehner, B.; Bräsel, S.; Hermann, M.; Stratmann, F.; Kulmala, M.; Wiedensohler, A. Dilution and aerosol dynamics within a diesel car exhaust plume—CFD simulations of on-road measurement conditions. *Atmos. Environ.* **2007**, *41* (35), 7440−7461.
(42) Gran, I. R.; Magnussen, B. F. A Numerical Study of a Bluff-Body Stabilized Diffusion Flame. Part 2. Influence of Combustion Modeling And Finite-Rate Chemistry. *Combust. Sci. Technol.* **1996**, *119* (1−6), 191−217.
(43) Magnussen, B. F.; Hjertager, B. H. In On mathematical modeling of turbulent combustion with special emphasis on soot formation and combustion, *Symposium (International) on Combustion*; Elsevier, 1977; pp 719−729.
(44) Yarwood, G.; Rao, S.; Yocke, M.; Whitten, G. *Updates to the carbon bond chemical mechanism: CB05*; RT-04-00675, 2005.
(45) Karamchandani, P.; Koo, A.; Seigneur, C. Reduced Gas-Phase Kinetic Mechanism for Atmospheric Plume Chemistry. *Environ. Sci. Technol.* **1998**, *32* (11), 1709−1720.
(46) CERC. *ADMS-Roads Air Quality Management System Version 4.1 User Guide*; Cambridge Environmental Research Consultants, 2017.
(47) Benson, P. E. A Review of the Development and Application of the CALIN3 and 4 Models. *Atmos. Environ.* **1992**, *26B* (3), 379−390.
(48) USEPA. *User's Guide for the AMS/EPA Regulatory Model (AERMOD)*; EPA-454/B-16-011; Office of Air Quality Planning and Standards, U.S. Environmental Protection Agency, 2016.
(49) Degraeuwe, B.; Thunis, P.; Clappier, A.; Weiss, M.; Lefebvre, W.; Janssen, S.; Vranckx, S. Impact of passenger car NO_X emissions on urban NO2 pollution − Scenario analysis for 8 European cities. *Atmos. Environ.* **2017**, *171*, 330−337.

DOI: 10.1021/acs.est.7b05648
Environ. Sci. Technol. 2018, 52, 4574−4582